



Association of epicardial adipose tissue volume with increased risk of hemodynamically significant coronary artery disease

Wenji Yu^{1,2}, Yongjun Chen^{3#}, Feifei Zhang^{1,2}, Bao Liu^{1,2}, Jianfeng Wang^{1,2}, Xiaoliang Shao^{1,2}, Xiaoyu Yang³, Yunmei Shi^{1,2}, Yuetao Wang^{1,2#^}

¹Department of Nuclear Medicine, The Third Affiliated Hospital of Soochow University, Changzhou, China; ²Institute of Clinical Translation of Nuclear Medicine and Molecular Imaging, Soochow University, Changzhou, China; ³Department of Cardiology, The Third Affiliated Hospital of Soochow University, Changzhou, China

Contributions: (I) Conception and design: W Yu, Y Wang; (II) Administrative support: Y Wang, Y Chen; (III) Provision of study materials or patients: X Yang, Y Chen; (IV) Collection and assembly of data: F Zhang, B Liu, Y Shi; (V) Data analysis and interpretation: J Wang, X Shao; (VI) Manuscript writing: All authors; (VII) Final approval of manuscript: All authors.

#These authors contributed equally to this work.

Correspondence to: Yongjun Chen, MD. Department of Cardiology, The Third Affiliated Hospital of Soochow University, No. 185, Juqian Street, Changzhou 213003, China. Email: cyjcz75@163.com; Yuetao Wang, MD. Department of Nuclear Medicine, The Third Affiliated Hospital of Soochow University, No.185, Juqian Street, Changzhou 213003, China. Email: yuetao-w@163.com.

Background: Epicardial adipose tissue (EAT) is closely related to coronary artery disease (CAD). Hemodynamically significant CAD has a worse prognosis and is more likely to benefit from revascularization. However, the specific relationship between EAT and hemodynamically significant CAD remains unclear.

Methods: A total of 164 inpatients received single-photon emission computerized tomography-myocardial perfusion imaging (SPECT/MPI) and coronary angiography (CAG) between March 2018 and October 2019 at the Third Affiliated Hospital of Soochow University were enrolled in the retrospective cross-sectional study. Data on body mass index (BMI), hypertension, hyperlipidemia, diabetes mellitus (DM), active smoking, and symptoms were gathered. Epicardial fat volume (EFV) and coronary artery calcium (CAC) were quantified by noncontrast computed tomography (CT). Hemodynamically significant CAD was defined by coronary stenosis severity $\geq 50\%$ with reversible perfusion defects in the corresponding areas of SPECT/MPI.

Results: A total of 37.8% of patients had hemodynamically significant CAD. Age and BMI increased with tertiles of EFV (P for trend =0.009 and P<0.001). The ratios of hemodynamically significant CAD in EFV from low to high were 16.4%, 37.0%, and 60.0%, respectively (P for the trend <0.001). In univariate regression analysis, EFV was associated with hemodynamically significant CAD [odds ratio (OR) per 10 cm³ =1.36; 95% confidence interval (CI): 1.20–1.55; P<0.001]. After correcting for traditional risk factors and CAC, EFV was firmly linked to hemodynamically significant CAD (OR per 10 cm³ =1.53; 95% CI: 1.25–1.88; P<0.001). With an increasing trend in EFV for the tripartite groups, the likelihood of hemodynamically significant CAD increased significantly (P for trend <0.001). There was a saturation effect between EFV and hemodynamically significant CAD according to the generalized additive model (GAM). When EFV <134.43 cm³, EFV was linearly correlated with hemodynamically significant CAD (OR per 10 cm³ =2.06; 95% CI: 1.45–2.94; P<0.001). When EFV ≥ 134.43 cm³, the hemodynamically significant CAD risk was steeper and gradually reached saturation. Hypertension affected the relationship between EFV and hemodynamically significant CAD (P for the interaction =0.02) with an interaction effect.

[^] ORCID: 0000-0003-2859-8625.

Conclusions: There was a robust relationship between EFV and hemodynamically significant CAD. After adjustment for confounders, we found that the risk of hemodynamically significant CAD onset increased nonlinearly for EFV above 134.4 cm³. This refined understanding of the relationship is helpful for the accurate clinical prediction of hemodynamically significant CAD.

Keywords: Epicardial fat volume (EFV); coronary artery calcium (CAC); coronary artery disease (CAD); myocardial ischemia; noncontrast CT

Submitted Jul 05, 2022. Accepted for publication Jan 20, 2023. Published online Feb 10, 2023.

doi: 10.21037/qims-22-709

View this article at: <https://dx.doi.org/10.21037/qims-22-709>

Introduction

Coronary artery disease (CAD) is the major cause of mortality in Chinese residents and has become a serious threat to national health (1). Coronary angiography (CAG) is accepted as a gold standard for diagnosing and treating CAD. However, the anatomically based assessment has significant deficiencies. CAD is the major cause of myocardial ischemia. When myocardial ischemia occurs in CAD patients, the incidence of major adverse cardiovascular events (MACEs) is much higher (2). Patients with CAD should undergo revascularization if myocardial ischemia is present (3). Single-photon emission computerized tomography-myocardial perfusion imaging (SPECT-MPI) is a noninvasive imaging technique to accurately diagnose myocardial ischemia with mature technology and sufficient evidence-based medicine (4). A combination of CAG and MPI can accurately diagnose myocardial ischemia associated with CAD, which is also known as hemodynamically significant CAD. However, CAG is an invasive test, and SPECT-MPI has a certain risk of radiation exposure. Thus, exploring a noninvasive and simple marker to predict hemodynamically significant CAD has important clinical significance for risk stratification, diagnosis and treatment decisions, and providing reliable prognostic information in patients with suspected CAD.

Recently, organ-specific adiposity has attracted increasing attention, especially epicardial adipose tissue (EAT), which can secrete varieties of cytokines and adipokines and damage the myocardium and coronary arteries (5,6). Noncontrast computed tomography (CT) scans can quantitatively assess coronary artery calcium (CAC) and measure epicardial fat volume (EFV). There has been considerable interest in the relationship between EFV and traditional risk factors, CAC, obstructive CAD, myocardial ischemia, and hemodynamically significant CAD; however, research in this area has been

controversial (7-9). A large population-based, multicenter study abroad highlighted significant ethnic differences in EFV (10). Our previous study confirmed that EAT was an independent risk factor for obstructive CAD (11), and myocardial ischemia has been significantly predicted by EFV over conventional risk factors and CAC (12). However, the specific relationship between EFV and hemodynamically significant CAD remains unclear. A refined comprehension of the correlation between EAT and hemodynamically CAD may provide insight into predicting hemodynamically CAD and thus contribute to identifying better therapeutic strategies.

In this study, noncontrast CT scans were used to quantify EFV and investigate the association between EFV and hemodynamically significant CAD. We present the following article in accordance with the STROBE reporting checklist (available at <https://qims.amegroups.com/article/view/10.21037/qims-22-709/rc>).

Methods

Study population

This retrospective cross-sectional study evaluates the relationship between EFV and hemodynamically significant CAD. The retrospective nature of the study included a predetermined sample size. We consecutively enrolled 164 inpatients who underwent SPECT/MPI and CAG with suspected CAD between March 2018 and October 2019 at the Third Affiliated Hospital of Soochow University. CAG was conducted within 3 months of MPI in all patients. Data on body mass index (BMI), hypertension, hyperlipidemia, diabetes mellitus (DM), active smoking, and symptom (angina, dyspnea, etc.) were gathered as traditional cardiovascular risk factors, which were defined as previously described by our team (11,12). Patients without symptoms were not completely asymptomatic but often had hidden

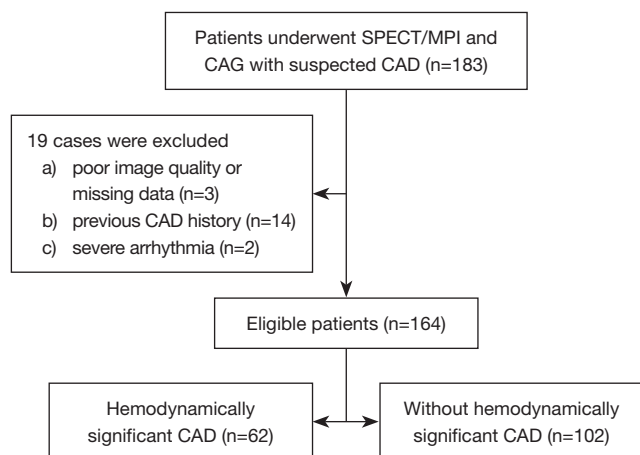


Figure 1 Patient selection flowchart. SPECT/MPI, single-photon emission computerized tomography-myocardial perfusion imaging; CAG, coronary angiography; CAD, coronary artery disease.

and easily ignored CAD-related symptoms, such as ectopic pain in the throat, teeth, neck, upper abdomen, shoulder and back, left forearm, and even in the lower limbs. They usually had cardiovascular risk factors (i.e., hypertension, DM, hyperlipidemia, smoking, being overweight, being ≥ 45 years old, and being women ≥ 55 years old), and hematologic examination or electrocardiographic abnormality identified during medical examinations. *Figure 1* shows the exclusion criteria and the study flowchart. The study was conducted in accordance with the Declaration of Helsinki (as revised in 2013). The Ethics Committee of the Third Affiliated Hospital of Soochow University approved the study protocol, and the requirement for informed consent was waived due to the retrospective nature of the study.

SPECT-MPI image acquisition and analysis

Twenty-four hours before testing, nitrates and beta-blockers were prohibited. Based on the recommendations of the relevant guidelines and 2-day standard imaging protocol, each patient underwent a gated stress-rest MPI (13). The scanning started 60–90 minutes after intravenous injection of a dose of 740–925 MBq ^{99m}Tc -MIBI, which has radiochemical purity $>95\%$. Our previous study provided the specific scan parameters (11). SPECT-MPI images were visually interpreted by 2 nuclear cardiologists (JF Wang and XL Shao, who were attending physicians) who were blinded to patients' clinical data. A third expert (YT Wang, chief physician) was invited when the conclusion was disputed, and then the consensus result was determined.

Corresponding to different coronary blood supply areas, the myocardial perfusion images were divided into 17 segments and scored on a 5-point scale, as explained in detail in our previous studies (11,12). The summed stress score (SSS) and summed rest score (SRS) were the sum of the 17-segment stress or resting perfusion scores. The summed difference score (SDS) equaled SSS minus SRS. The definition of myocardial ischemia is a reversible perfusion defect with $\text{SDS} \geq 2$ (14).

Image acquisition and analysis of CAC and EFV

A low-dose noncontrast CT chest scan was performed after tomographic image acquisition for stress MPI. Our previous study provides the specific scan parameters (11). Approximately 20 cm were scanned from the tracheal carina diaphragmatic surface of the heart to 1 cm beneath the plane underneath the tracheal carina.

CAC was defined as the presence of at least 3 contiguous pixels with a density surpassing 130 Hounsfield unit (HU) and was determined with Agatston automatic analysis software (Syngo Casoring, Siemens Healthineers, Erlangen, Germany) (15).

EAT was defined as the adipose tissue between the myocardium and the pericardium with a window width of -190 to -30 HU. EAT was manually delineated from the bifurcation of the pulmonary trunk to the level of the diaphragm by layer at 5-mm intervals with the reconstructed axial slices. Using Syngo Volume (Siemens Healthineers), we calculated the EFV as the sum of the cross-sectional areas of fat multiplied by the slice thickness with the noncontrast CT scan (16). The intraclass correlation coefficient for EFV was 0.96 [95% confidence interval (CI): 0.89–0.98; $P < 0.001$].

CAG

CAG was performed through the radial approach and interpreted by 2 experienced cardiologists independently (XY Yang and YJ Chen, who were attending physicians). Obstructive CAD was defined as $\geq 50\%$ stenosis in at least 1 of the major epicardial coronary arteries (17).

Diagnosis of hemodynamically significant CAD

Hemodynamically significant CAD was defined as (I) coronary stenosis severity $\geq 50\%$ and (II) reversible perfusion defects in the corresponding areas of SPECT-MPI. If none or 1 of the above criteria was satisfied, this was

Table 1 Baseline characteristics stratified by tertiles of EFV

Characteristics	Bottom tertile	Middle tertile	Top tertile	P value for trend
EFV (cm ³), range	37.30–107.36	107.36–128.49	128.49–246.49	
EFV (cm ³), mean ± SD	83.34±18.69	117.06±6.60	157.97±28.31	
EFV (cm ³), median (IQR)	84.80 (31.32)	114.49 (12.01)	144.63 (34.68)	
Age (years), mean ± SD	58.18±10.62	62.28±8.81	63.73±9.62	0.009*
Male, n (%)	40 (72.7)	34 (63.0)	37 (67.3)	0.550
BMI (kg/m ²), mean ± SD	22.98±2.86	24.93±2.35	26.38±2.96	<0.001*
Symptom, n (%)	33 (60.0)	35 (64.8)	40 (72.7)	0.36
Active smoking, n (%)	19 (34.5)	14 (25.9)	21 (38.2)	0.38
Hypertension, n (%)	32 (58.2)	40 (74.1)	41 (74.5)	0.11
Diabetes mellitus, n (%)	13 (23.6)	17 (31.5)	22 (40.0)	0.18
Hyperlipidemia, n (%)	15 (27.3)	14 (25.9)	24 (43.6)	0.09
CAC prevalence, n (%)	25 (45.5)	28 (51.9)	27 (49.1)	0.80
Hemodynamically significant CAD, n (%)	9 (16.4)	20 (37.0)	33 (60.0)	<0.001*

*, P for trend <0.05. EFV, epicardial fat volume; SD, standard deviation; IQR, interquartile range; BMI, body mass index; Symptom, angina, dyspnea, atypical chest pain, and dyspnea with angina or atypical chest pain; CAC, coronary artery calcium; CAD, coronary artery disease.

defined as without hemodynamically significant CAD.

Radiation exposure

The effective radiation dose received by patients during the whole scanning process was 10–14 mSv (9–12 mSv for SPECT/MPI, and 1–2 mSv for noncontrast CT).

Statistical analysis

Continuous variables with a normal distribution are expressed as mean ± standard deviation (SD); otherwise, they are expressed as a median (25–75th percentile). The Mann-Whitney test, independent samples *t*-test, and χ^2 test were conducted according to the appropriate paradigm. Using trend tests, we illustrated the influencing factors associated with the tertiles of EFV. The relationships between the characteristics and hemodynamically significant CAD were evaluated using univariate logistic regression analysis. Three models were created to determine the relationship between EFV and hemodynamically significant CAD, including unadjusted, preliminarily adjusted, and fully adjusted models based on our team's interpretation of a broad literature review. Covariates were included as potential confounders in the model if they changed

the estimates of EFV on hemodynamically significant CAD by more than 10% or were significantly related to hemodynamically significant CAD ($P < 0.10$) (18). EFV was converted into categorical variables using 3 equal division ratios, and P values for trends were calculated to test the robustness of the results as a sensitivity analysis. A generalized additive model (GAM) and smooth curve fitting were used to test whether there was a nonlinear relationship, and a piecewise binary logistic regression model was used to explain nonlinearity (19). A hierarchical binary logistic regression model was used to assess whether there was an interaction effect on the relationship between EFV and hemodynamically significant CAD in different subgroups. All tests were performed 2-sided with the following R 3.4.3 (<http://www.R-project.org>) software packages: “glmnet”, “pROC”, “rms”, and “dca”. A P value less than 0.05 was considered significant.

Results

A general overview of EFV tertiles

Table 1 demonstrates the influence factors of tripartite EFV. There were 55 cases in tertile 1 (EFV: 37.30–107.36 cm³), 54 cases in tertile 2 (EFV: 107.36–128.49 cm³), and 55 cases

Table 2 Crude association between risk factors and hemodynamically significant CAD

Characteristics	Statistic, n (%) or mean \pm SD	OR (95% CI)	P value
Male	111 (67.7)	1.44 (0.72–2.88)	0.30
Age (years)	61.39 \pm 9.94	1.02 (0.99–1.06)	0.18
BMI (kg/m ²)	24.76 \pm 3.06	1.14 (1.02–1.27)	0.02*
Active smoking	54 (32.9)	1.07 (0.55–2.09)	0.84
Hypertension	113 (68.9)	3.49 (1.60–7.66)	0.002*
Hyperlipidemia	53 (32.3)	1.42 (0.73–2.76)	0.31
Diabetes mellitus	52 (31.7)	1.87 (0.96–3.67)	0.06
Symptom	108 (65.9)	2.75 (1.33–5.68)	0.006*
CAC	80 (48.8)	7.50 (3.62–15.53)	<0.001*
EFV (per 10 cm ³)	116.69 \pm 35.15	1.36 (1.20–1.55)	<0.001*

*, P<0.05. CAD, coronary artery disease; OR, odd ratio; CI, confidence interval; SD, standard deviation; BMI, body mass index; Symptom, angina, dyspnea, atypical chest pain, and dyspnea with angina or atypical chest pain; CAC, coronary artery calcium; EFV, epicardial fat volume; SD, standard deviation.

in tertile 3 (EFV: 128.49–246.49 cm³). Age, BMI, and incidences of hemodynamically significant CAD were increased with tertiles of EFV (trend P=0.009, P<0.001, and P<0.001, respectively). The proportions of hemodynamically significant CAD in the EFV of low, middle, and high were 16.4%, 37.0%, and 60.0%, respectively.

Crude association between risk factors and hemodynamically significant CAD

Among the 164 patients enrolled, there were 111 males, the mean age was 61.39 \pm 9.94 years, the mean BMI was 24.76 \pm 3.06 kg/m², and the mean EFV was 116.7 cm³. A total of 80 (80/164, 48.8%) patients had CAC, and 62 (62/164, 37.8%) had hemodynamically significant CAD. We used hemodynamically significant CAD as the dependent variable (Y=1) and traditional risk factors, CAC, and EFV as the independent variables to conduct the univariate logistic regression analysis. BMI, hypertension, symptom, CAC, and EFV were related to hemodynamically significant CAD (P=0.02, P=0.002, P=0.006, P<0.001, and P<0.001, respectively; *Table 2*).

Multivariable logistic regression analysis on the effect of the EFV on hemodynamically significant CAD

An analysis of logistic regressions for continuous and categorical EFV is shown in *Table 3*. Adjust I covariates

included BMI, symptoms, DM, hypertension, and CAC. Fully adjusted (adjust II) covariates included age, gender, BMI, hypertension, DM, active smoking, hyperlipidemia, symptom, and CAC prevalence. For continuous EFV, a 10 cm³ increase in EFV was related to an elevated risk of hemodynamically significant CAD in the unadjusted, adjust I, and adjust II regression models, and the odds ratios (ORs) were 1.36, 1.46, and 1.53, respectively (all P values <0.001). For categorical EFV, there was also a significant correlation between increasing EFV and hemodynamically significant CAD in the unadjusted, adjust I, and adjust II regression models (P values for all trends <0.001), particularly when the comparing the high and low tertile (ORs =7.67, 10.00, and 17.32, respectively; all P values <0.001).

Curve fitting and threshold saturation effect

GAM was used to test the relationship between EFV and hemodynamically significant CAD. The results showed that, with the increase of EFV, the risk of hemodynamically significant CAD showed a significant increase at first and then tended to be flat, exhibiting a piecewise linear relationship after adjustment for traditional risk factors and CAC prevalence (*Figure 2A*). When EFV was processed as tertiles, the adjusted mean probability of hemodynamically significant CAD increased with tertiles of EFV, which was 16.4% (95% CI: 4.6–44.3%), 39.6% (95% CI: 16.7–68.3%), and 77.2% (95% CI: 48.8–92.3%) from tertile 1 to tertile 3,

Table 3 Multivariate regression analysis for the effect of EFV on hemodynamically significant CAD

Variables	Nonadjusted		Adjusted I		Adjusted II	
	OR (95% CI)	P value	OR (95% CI)	P value	OR (95% CI)	P value
EFV (per 10 cm ³)	1.36 (1.20–1.55)	<0.001	1.46 (1.20–1.77)	<0.001	1.53 (1.25–1.88)	<0.001
Tertiles						
Bottom tertile (events/n=9/55)	1		1		1	
Middle tertile (events/n=20/54)	3.01 (1.22–7.42)	0.02	2.57 (0.83–7.95)	0.10	3.35 (1.00–11.20)	0.049
Top tertile* (events/n=33/55)	7.67 (3.13–18.77)	<0.001	10.00 (2.76–36.24)	<0.001	17.32 (3.95–75.89)	<0.001

Adjusted I, model adjusted for BMI, hypertension, DM, symptom, and coronary artery calcium prevalence; Adjusted II, model adjusted for age, gender, BMI, hypertension, DM, active smoking, hyperlipidemia, symptom, and coronary artery calcium prevalence; *, P for trend <0.001. EFV, epicardial fat volume; CAD, coronary artery disease; OR, odds ratio; CI, confidence interval.

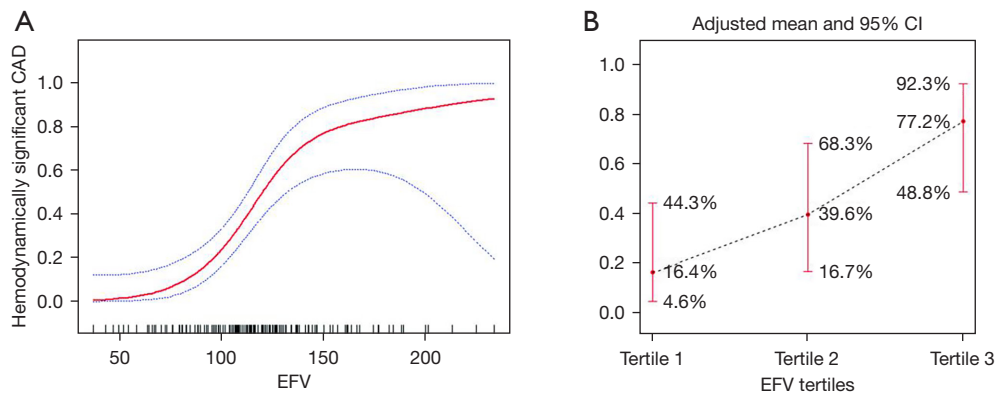


Figure 2 The general additive model demonstrates the relationship between EFV and the risk of hemodynamically significant CAD. (A) The relationship between EFV and hemodynamically significant CAD (the solid red line indicates the fitted line; the blue dotted lines are the 95% confidence interval), adjusted for age, gender, BMI, hypertension, DM, active smoking, hyperlipidemia, symptom, and CAC prevalence. (B) The relationship between EFV tertiles and hemodynamically significant CAD (the black dotted line indicates the fitted line; the red line is the 95% CI), adjusted for age, gender, BMI, hypertension, DM, active smoking, hyperlipidemia, typical symptom, and CAC prevalence. CAD, coronary artery disease; EFV, epicardial fat volume; CI, confidence interval; CAC, coronary artery calcium; BMI, body mass index; DM, diabetes mellitus.

Table 4 Threshold effect analysis of EFV on hemodynamically significant CAD using piecewise linear regression

Inflection point of EFV	Effect size (OR, per 10 cm ³)	95% CI	P value
<134.43 cm ³	2.06	1.45–2.94	<0.001
≥134.43 cm ³	1.06	0.76–1.47	0.73

EFV, epicardial fat volume; CAD, coronary artery disease; OR, odds ratio; CI, confidence interval.

respectively (Figure 2B).

The fitting curve was further evaluated by a piecewise logistic regression model to determine if there was a saturation effect after adjustment for traditional risk factors and CAC. The results showed that when the EFV was 134.43 cm³, the log-likelihood ratio test results were statistically significant (P=0.014) and that the piecewise regression model should be applied (Table 4). When the

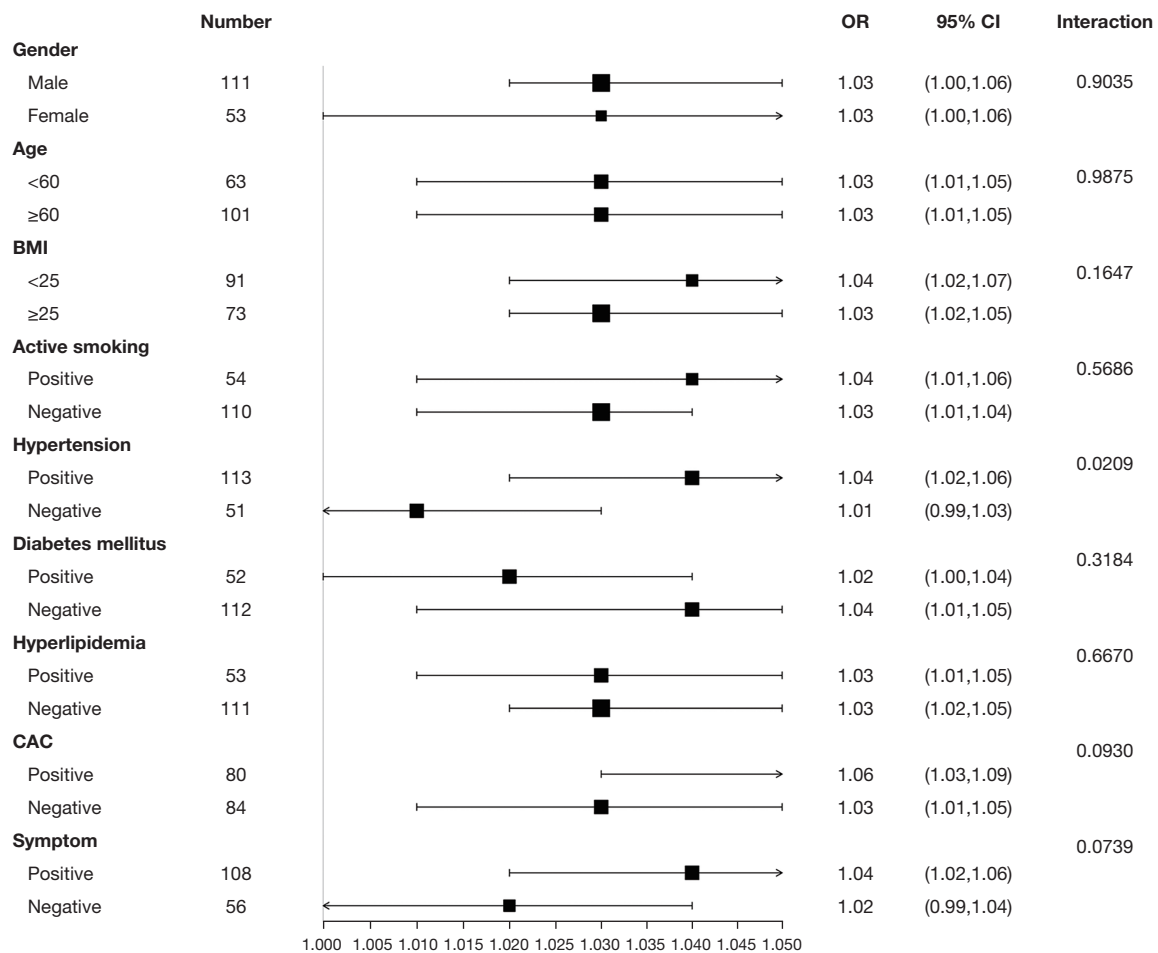


Figure 3 Stratification analysis of EFV and hemodynamically significant CAD. BMI, body mass index; CAC, coronary artery calcium; OR, odds ratio; CI, confidence interval; EFV, epicardial fat volume; CAD, coronary artery disease.

EFV was $<134.43 \text{ cm}^3$, the EFV was linearly associated with the risk of hemodynamically significant CAD. With each additional 10 cm^3 of EFV, there was a 1.06-fold increase in the risk of hemodynamically significant CAD (OR per $10 \text{ cm}^3 = 2.06$; 95% CI: 1.45–2.94; $P < 0.001$). In contrast, $\text{EFV} \geq 134.43 \text{ cm}^3$ showed a steeper risk of hemodynamically significant CAD and a saturation effect (OR per $10 \text{ cm}^3 = 1.06$; 95% CI: 0.76–1.47; $P = 0.73$).

Stratified analysis

The relationship between EFV and hemodynamically significant CAD in each subgroup was further evaluated by stratified analysis, including age, gender, BMI, hypertension, DM, active smoking, hyperlipidemia, symptom, and CAC prevalence (Figure 3). The interaction analysis revealed that

hypertension played an interactive role in the relationship between EFV and hemodynamically significant CAD. The P value for interaction was 0.02. Further analysis found that the OR value of EFV and hemodynamically significant CAD in the hypertension subgroup was 1.04 (95% CI: 1.02–1.06; $P < 0.001$). The characteristics of the hypertension groups are compared in Supplementary Material Table S1. No other variables significantly changed the association between EFV and hemodynamically significant CAD (interaction: $P = 0.90$, $P = 0.99$, $P = 0.16$, $P = 0.57$, $P = 0.32$, $P = 0.67$, $P = 0.09$, and $P = 0.07$, respectively).

Discussion

The main findings of the study were as follows. First, age, BMI, and incidences of hemodynamically significant CAD

increased with tertiles of EFV. Second, each 10 cm³ increase in EFV raised the risk of hemodynamically significant CAD by 53% after adjustment for traditional risk factors and CAC. Third, after the adjustment for confounders, the risk of hemodynamically significant CAD onset increased nonlinearly for EFV above 134.4 cm³. Fourth, the interaction analysis revealed that hypertension played an interactive role in the association between EFV and hemodynamically significant CAD.

We found that EFV was independently related to hemodynamically significant CAD. The mechanisms underlying the association between EFV and hemodynamically significant CAD are complicated and not thoroughly elucidated. Potential mechanisms include inflammatory response, oxidative stress, impairment of the endothelium, influence of coronary blood flow, and damage to the microcirculation, among others (20-22). Previous investigations evaluated the relationship between EFV and hemodynamically significant CAD, but the results were controversial. Brandt *et al.* (23) demonstrated that EFV was significantly higher in patients with hemodynamically significant CAD compared to patients without hemodynamically significant CAD as detected by fractional flow reserve (FFR). Although FFR was found to quantitatively reflect flow limitation caused by coronary artery stenosis, it was not considered suitable for clinical screening. Romijn *et al.* (24) also found that EFV was independently associated with hemodynamically significant CAD in a multivariable-adjusted model (OR: 4.95; 95% CI: 1.31–18.6; P=0.02). However, FFR was only performed in 32% of patients, which might have overestimated the effect of EFV. Furthermore, Nakazato *et al.* (25) found that indexed EFV (EFVi) predicted the concurrent presence of both myocardial ischemia and obstructive stenosis. We used SPECT-MPI to detect myocardial ischemia instead of positron emission tomography-computed tomography (PET-CT), which is more clinically practiced. In contrast, Muthalaly *et al.* (26) demonstrated there to be no observable relationship between EFV and functionally significant stenosis as detected with myocardial CT perfusion imaging, as well as invasive FFR. Since EAT is influenced by a large number of factors, without adjusted analyses, the study was unable to confirm the independent relationship between EAT and hemodynamically significant CAD. Tanami *et al.* (10) also did not find there to be association between EFV, the severity of CAD, or the presence of myocardial perfusion abnormalities. The study also highlighted significant ethnic differences in EFV.

We extended information gained from those investigations in Chinese patients with suspected CAD by evaluating the specific relationship. We found that there was nonlinear relationship between EFV and hemodynamically significant CAD after fully correcting the confounding and interaction factors; more specifically, a significant positive linear correlation existed between the 2 within a certain threshold range, then the trend flattened, and a saturation effect occurred when the threshold was exceeded. The cutoff value was 134.43 cm³, and this result provided a preliminary basis for the subsequent development of clinical prediction models. This nonlinear relationship suggests that subsequent studies may better use a nonlinear model, such as multivariate fractional polynomials (MFP), for predicting hemodynamically significant CAD (27). We also divided the EFV into 3 equal parts. With the increase of the EFV levels, the probability of hemodynamically significant CAD still had a similar trend, indicating that the relationship was robust.

Through stratified analysis, we found hypertension had an interactive role in the relationship between EFV and hemodynamically significant CAD. The different characteristics of the hypertension subgroups may account for the interaction effect. The hypertension subgroup had a large sample size (n=113), which may account for the more significant relationship between EFV and hemodynamically significant CAD. Hypertension is an important risk factor associated with obesity (28). It has been reported that patients with hypertension have lower levels of EAT messenger RNA expression of adiponectin (29). It is also well known that hypoadiponectinemia is a risk factor for CAD (30). A stronger association between EFV and hemodynamically significant CAD in hypertensive populations could be associated with the decline of the protective endocrine and the local paracrine effects of adiponectin.

Hemodynamically significant CAD is clinically significant in patients, as they will have a worse prognosis and are more likely to benefit from revascularization (31). Therefore, it is necessary to find simplified, innovative, reproducible, and noninvasive cardiovascular risk markers of hemodynamically significant CAD to improve risk stratification and guide clinical treatment decision-making. Besides EAT, several investigations focused on pericoronary adipose tissue (PCAT) and evaluated the relationship with hemodynamically significant CAD. Ma *et al.* (32) found that a lesion-specific fat attenuation index was independently associated with abnormal FFR. However, Wen *et al.* (33) indicated that PCAT had no merit in identifying hemodynamically

significant coronary stenosis. Moreover, it has been reported that volumetric quantification of EAT was highly reproducible compared to more simple measurements, such as pericoronary fat thickness and area (34). The repeatability of EFV measurements was notably high in the present study. Thus, measuring EFV, the global information of EAT, with noncontrast CT and without extra protocols or radiation exposure is still helpful for the initial screening of high-risk, hemodynamically significant CAD because it can facilitate clinical decision-making and risk stratification more safely. Moreover, Alam *et al.* (35) concluded that EAT is related to vessel inflammation and microcirculation dysfunction. Another study also found that EFV could effectively predict a patient's long-term MACE risk (36). The clinical significance of EFV is worth evaluating in further prospective studies.

Limitations

In the present study, we had several limitations. First, as our study was retrospectively designed, we were unable to infer causal relationships. Only enrolling inpatients undergoing CAD testing might have resulted in selection bias, and low-risk individuals may not be represented. Prospective, multicenter studies are still needed to support the effect of EAT on hemodynamically significant CAD. Second, automatic software is still necessary to make EFV clinically practicable. This study did not measure the pericoronary fat, and we will quantitatively measure the pericoronary fat in the future to evaluate its application in CAD. Third, there are no standardized quantitative categories for EFV. There are significant racial differences in EAT; therefore, it is necessary to improve the relevant database of EAT in the Chinese population and find the appropriate threshold to assist further risk stratification, diagnosis, and treatment decisions of cardiovascular diseases. Finally, follow-up is required to expand the sample size to evaluate the effect of EFV on the prognosis of hemodynamically significant CAD. In a follow-up study, the sample size will be expanded to further explore the practicality and feasibility of using EFV as a gatekeeper prior to CAG or SPECT-MPI.

Conclusions

There was a robust relationship between EFV and hemodynamically significant CAD independent of traditional risk factors and CAC. After adjustment for confounders, there was a nonlinear relationship,

saturation, and segmentation effects between EFV and hemodynamically significant CAD, with a steeper risk in incidence rates noted for values over 134.4 cm³. Understanding and recognizing the relationship between EFV and hemodynamically significant CAD may help improve the accuracy of diagnosis and develop more specific predictive models.

Acknowledgments

Funding: This research was supported by the National Natural Science Foundation of China [No. 82272031; principal investigator (PI): Yuetao Wang], the Key Research and Development Program of Jiangsu Province (Social Development; No. BE2021638), The Science and Technology Project for Youth Talents of Changzhou Health Committee (No. QN202212; PI: Wenji Yu).

Footnote

Reporting Checklist: The authors have completed the STROBE reporting checklist. Available at <https://qims.amegroups.com/article/view/10.21037/qims-22-709/rc>

Conflicts of Interest: All authors have completed the ICMJE uniform disclosure form (available at <https://qims.amegroups.com/article/view/10.21037/qims-22-709/coif>). The authors have no conflicts of interest to declare.

Ethical Statement: The authors are accountable for all aspects of the work in ensuring that questions related to the accuracy or integrity of any part of the work are appropriately investigated and resolved. The study was conducted in accordance with the Declaration of Helsinki (as revised in 2013). The Ethics Committee of the Third Affiliated Hospital of Soochow University approved the study protocol, and the requirement for informed consent was waived due to the retrospective nature of the study.

Open Access Statement: This is an Open Access article distributed in accordance with the Creative Commons Attribution-NonCommercial-NoDerivs 4.0 International License (CC BY-NC-ND 4.0), which permits the non-commercial replication and distribution of the article with the strict proviso that no changes or edits are made and the original work is properly cited (including links to both the formal publication through the relevant DOI and the license). See: <https://creativecommons.org/licenses/by-nc-nd/4.0/>.

References

1. Ma LY, Chen WW, Gao RL, Liu LS, Zhu ML, Wang YJ, Wu ZS, Li HJ, Gu DF, Yang YJ, Zheng Z, Hu SS. China cardiovascular diseases report 2018: an updated summary. *J Geriatr Cardiol* 2020;17:1-8.
2. Kattoor AJ, Kolkailah AA, Iskander F, Iskander M, Diep L, Khan R, Doukky R. The prognostic value of regadenoson SPECT myocardial perfusion imaging: The largest cohort to date. *J Nucl Cardiol* 2021;28:2799-807.
3. Ornish D, Redberg RF. PCI Guided by Fractional Flow Reserve at 5 Years. *N Engl J Med* 2019;380:103-4.
4. Wolk MJ, Bailey SR, Doherty JU, Douglas PS, Hendel RC, Kramer CM, Min JK, Patel MR, Rosenbaum L, Shaw LJ, Stainback RF, Allen JM; . ACCF/AHA/ASE/ASNC/HFSA/HRS/SCAI/SCCT/SCMR/STS 2013 multimodality appropriate use criteria for the detection and risk assessment of stable ischemic heart disease: a report of the American College of Cardiology Foundation Appropriate Use Criteria Task Force, American Heart Association, American Society of Echocardiography, American Society of Nuclear Cardiology, Heart Failure Society of America, Heart Rhythm Society, Society for Cardiovascular Angiography and Interventions, Society of Cardiovascular Computed Tomography, Society for Cardiovascular Magnetic Resonance, and Society of Thoracic Surgeons. *J Am Coll Cardiol* 2014;63:380-406.
5. Baker AR, Harte AL, Howell N, Pritlove DC, Ranasinghe AM, da Silva NF, Youssef EM, Khunti K, Davies MJ, Bonser RS, Kumar S, Pagano D, McTernan PG. Epicardial adipose tissue as a source of nuclear factor-kappaB and c-Jun N-terminal kinase mediated inflammation in patients with coronary artery disease. *J Clin Endocrinol Metab* 2009;94:261-7.
6. Mazurek T, Zhang L, Zalewski A, Mannion JD, Diehl JT, Arafat H, Sarov-Blat L, O'Brien S, Keiper EA, Johnson AG, Martin J, Goldstein BJ, Shi Y. Human epicardial adipose tissue is a source of inflammatory mediators. *Circulation* 2003;108:2460-6.
7. Mahabadi AA, Lehmann N, Möhlenkamp S, Pundt N, Dykun I, Roggenbuck U, Moebus S, Jöckel KH, Erbel R, Kälisch H; . Noncoronary Measures Enhance the Predictive Value of Cardiac CT Above Traditional Risk Factors and CAC Score in the General Population. *JACC Cardiovasc Imaging* 2016;9:1177-85.
8. Tamarappoo B, Dey D, Shmilovich H, Nakazato R, Gransar H, Cheng VY, Friedman JD, Hayes SW, Thomson LE, Slomka PJ, Rozanski A, Berman DS. Increased pericardial fat volume measured from noncontrast CT predicts myocardial ischemia by SPECT. *JACC Cardiovasc Imaging* 2010;3:1104-12.
9. Greco F, Salgado R, Van Hecke W, Del Buono R, Parizel PM, Mallio CA. Epicardial and pericardial fat analysis on CT images and artificial intelligence: a literature review. *Quant Imaging Med Surg* 2022;12:2075-89.
10. Tanami Y, Jinzaki M, Kishi S, Matheson M, Vavere AL, Rochitte CE, Dewey M, Chen MY, Clouse ME, Cox C, Kuribayashi S, Lima JA, Arbab-Zadeh A. Lack of association between epicardial fat volume and extent of coronary artery calcification, severity of coronary artery disease, or presence of myocardial perfusion abnormalities in a diverse, symptomatic patient population: results from the CORE320 multicenter study. *Circ Cardiovasc Imaging* 2015;8:e002676.
11. Yu W, Liu B, Zhang F, Wang J, Shao X, Yang X, Shi Y, Wang B, Xu Y, Wang Y. Association of Epicardial Fat Volume With Increased Risk of Obstructive Coronary Artery Disease in Chinese Patients With Suspected Coronary Artery Disease. *J Am Heart Assoc* 2021;10:e018080.
12. Yu W, Zhang F, Liu B, Wang J, Shao X, Yang MF, Yang X, Wu Z, Li S, Shi Y, Wang B, Xu Y, Wang Y. Incremental value of epicardial fat volume to coronary artery calcium score and traditional risk factors for predicting myocardial ischemia in patients with suspected coronary artery disease. *J Nucl Cardiol* 2022;29:1583-92.
13. Henzlova MJ, Duvall WL, Einstein AJ, Travin MI, Verberne HJ. ASNC imaging guidelines for SPECT nuclear cardiology procedures: Stress, protocols, and tracers. *J Nucl Cardiol* 2016;23:606-39.
14. Xu Y, Fish M, Gerlach J, Lemley M, Berman DS, Germano G, Slomka PJ. Combined quantitative analysis of attenuation corrected and non-corrected myocardial perfusion SPECT: Method development and clinical validation. *J Nucl Cardiol* 2010;17:591-9.
15. Xu C, Guo H, Xu M, Duan M, Wang M, Liu P, Luo X, Jin Z, Liu H, Wang Y. Automatic coronary artery calcium scoring on routine chest computed tomography (CT): comparison of a deep learning algorithm and a dedicated calcium scoring CT. *Quant Imaging Med Surg* 2022;12:2684-95.
16. Huang G, Wang D, Zeb I, Budoff MJ, Harman SM, Miller V, Brinton EA, El Khoudary SR, Manson JE, Sowers MR, Hodis HN, Merriam GR, Cedars MI, Taylor HS, Naftolin F, Lobo RA, Santoro N, Wildman RP. Intra-thoracic fat, cardiometabolic risk factors, and

- subclinical cardiovascular disease in healthy, recently menopausal women screened for the Kronos Early Estrogen Prevention Study (KEEPS). *Atherosclerosis* 2012;221:198-205.
17. Rochitte CE, George RT, Chen MY, Arbab-Zadeh A, Dewey M, Miller JM, et al. Computed tomography angiography and perfusion to assess coronary artery stenosis causing perfusion defects by single photon emission computed tomography: the CORE320 study. *Eur Heart J* 2014;35:1120-30.
 18. Jaddoe VW, de Jonge LL, Hofman A, Franco OH, Steegers EA, Gaillard R. First trimester fetal growth restriction and cardiovascular risk factors in school age children: population based cohort study. *BMJ* 2014;348:g14.
 19. van der Meer D, Sønderby IE, Kaufmann T, Walters GB, Abdellaoui A, et al. Association of Copy Number Variation of the 15q11.2 BP1-BP2 Region With Cortical and Subcortical Morphology and Cognition. *JAMA Psychiatry* 2020;77:420-30.
 20. Sacks HS, Fain JN. Human epicardial adipose tissue: a review. *Am Heart J* 2007;153:907-17.
 21. Packer M. Epicardial Adipose Tissue May Mediate Deleterious Effects of Obesity and Inflammation on the Myocardium. *J Am Coll Cardiol* 2018;71:2360-72.
 22. Iacobellis G. Local and systemic effects of the multifaceted epicardial adipose tissue depot. *Nat Rev Endocrinol* 2015;11:363-71.
 23. Brandt V, Decker J, Schoepf UJ, Varga-Szemes A, Emrich T, Aquino G, Bayer RR 2nd, Carson L, Sullivan A, Ellis L, von Knebel Doeberitz PL, Ebersberger U, Bekeredjian R, Tesche C. Additive value of epicardial adipose tissue quantification to coronary CT angiography-derived plaque characterization and CT fractional flow reserve for the prediction of lesion-specific ischemia. *Eur Radiol* 2022;32:4243-52.
 24. Romijn MA, Danad I, Bakum MJ, Stuijzand WJ, Tulevski II, Somsen GA, Lammertsma AA, van Kuijk C, van de Ven PM, Min JK, Leipsic J, van Rossum AC, Raijmakers PG, Knaapen P. Incremental diagnostic value of epicardial adipose tissue for the detection of functionally relevant coronary artery disease. *Atherosclerosis* 2015;242:161-6.
 25. Nakazato R, Dey D, Cheng VY, Gransar H, Slomka PJ, Hayes SW, Thomson LE, Friedman JD, Min JK, Berman DS. Epicardial fat volume and concurrent presence of both myocardial ischemia and obstructive coronary artery disease. *Atherosclerosis* 2012;221:422-6.
 26. Muthalaly RG, Nerlekar N, Wong DT, Cameron JD, Seneviratne SK, Ko BS. Epicardial adipose tissue and myocardial ischemia assessed by computed tomography perfusion imaging and invasive fractional flow reserve. *J Cardiovasc Comput Tomogr* 2017;11:46-53.
 27. Löppenber B, Dalela D, Karabon P, Sood A, Sammon JD, Meyer CP, Sun M, Noldus J, Peabody JO, Trinh QD, Menon M, Abdollah F. The Impact of Local Treatment on Overall Survival in Patients with Metastatic Prostate Cancer on Diagnosis: A National Cancer Data Base Analysis. *Eur Urol* 2017;72:14-9.
 28. Teijeira-Fernandez E, Eiras S, Grigorian-Shamagian L, Fernandez A, Adrio B, Gonzalez-Juanatey JR. Epicardial adipose tissue expression of adiponectin is lower in patients with hypertension. *J Hum Hypertens* 2008;22:856-63.
 29. de Simone G, Mancusi C, Izzo R, Losi MA, Aldo Ferrara L. Obesity and hypertensive heart disease: focus on body composition and sex differences. *Diabetol Metab Syndr* 2016;8:79.
 30. Santaniemi M, Kesäniemi YA, Ukkola O. Low plasma adiponectin concentration is an indicator of the metabolic syndrome. *Eur J Endocrinol* 2006;155:745-50.
 31. Neumann FJ, Sousa-Uva M, Ahlsson A, Alfonso F, Banning AP, Benedetto U, et al. 2018 ESC/EACTS Guidelines on myocardial revascularization. *Eur Heart J* 2019;40:87-165.
 32. Ma S, Chen X, Ma Y, Liu H, Zhang J, Xu L, Wang Y, Liu T, Wang K, Yang J, Hou Y. Lesion-Specific Peri-Coronary Fat Attenuation Index Is Associated With Functional Myocardial Ischemia Defined by Abnormal Fractional Flow Reserve. *Front Cardiovasc Med* 2021;8:755295.
 33. Wen D, Li J, Ren J, Zhao H, Li J, Zheng M. Pericoronary adipose tissue CT attenuation and volume: Diagnostic performance for hemodynamically significant stenosis in patients with suspected coronary artery disease. *Eur J Radiol* 2021;140:109740.
 34. Gorter PM, van Lindert AS, de Vos AM, Meijs MF, van der Graaf Y, Doevendans PA, Prokop M, Visseren FL. Quantification of epicardial and peri-coronary fat using cardiac computed tomography; reproducibility and relation with obesity and metabolic syndrome in patients suspected of coronary artery disease. *Atherosclerosis* 2008;197:896-903.
 35. Alam MS, Green R, de Kemp R, Beanlands RS, Chow BJ. Epicardial adipose tissue thickness as a predictor of impaired microvascular function in patients with non-

- obstructive coronary artery disease. *J Nucl Cardiol* 2013;20:804-12.
36. Cheng VY, Dey D, Tamarappoo B, Nakazato R, Gransar H, Miranda-Peats R, Ramesh A, Wong ND, Shaw LJ,

Slomka PJ, Berman DS. Pericardial fat burden on ECG-gated noncontrast CT in asymptomatic patients who subsequently experience adverse cardiovascular events. *JACC Cardiovasc Imaging* 2010;3:352-60.

Cite this article as: Yu W, Chen Y, Zhang F, Liu B, Wang J, Shao X, Yang X, Shi Y, Wang Y. Association of epicardial adipose tissue volume with increased risk of hemodynamically significant coronary artery disease. *Quant Imaging Med Surg* 2023;13(4):2582-2593. doi: 10.21037/qims-22-709

Table S1 Characteristics of the different hypertension subgroups

	Hypertension (n=113)	Without hypertension (n=51)	P value
Male, n (%)	73 (64.6)	38 (74.5)	0.21
Age (years, mean \pm SD)	62.55 \pm 9.57	58.82 \pm 10.37	0.05
BMI (kg/m ² , mean \pm SD)	24.35 \pm 3.34	24.99 \pm 2.92	0.13
Active smoking, n (%)	34 (30.1)	20 (39.2)	0.25
Hyperlipidemia, n (%)	34 (30.1)	19 (27.3)	0.36
Diabetes mellitus, n (%)	36 (31.9)	16 (31.4)	0.95
Symptom, n (%)	73 (64.6)	35 (68.6)	0.62
EFV (cm ³ , mean \pm SD)	121.07 \pm 35.55	106.98 \pm 32.52	0.04*
CAC, n (%)	61 (54.0)	19 (37.2)	0.04*
Hemodynamically significant CAD, n (%)	52 (46.0)	10 (19.6)	0.001*

*, P for trend <0.05. EFV, epicardial fat volume; BMI, body mass index; CAC, coronary artery calcium; symptom, angina, dyspnea, atypical chest pain, and dyspnea with angina or atypical chest pain; SD, standard deviation.